Appl Phys A (2011) 104:289–294
DOI 10.1007/s00339-010-6127-9

Applied Physics A
Materials Science & Processing

Nondestructive 3-D imaging of femtosecond laser written volumetric structures using optical coherence microscopy

Jiyeon Choi · Kye-Sung Lee · Jannick P. Rolland · Troy Anderson · Martin C. Richardson

Received: 6 May 2010 / Accepted: 8 November 2010 / Published online: 8 December 2010

Abstract Nondestructive three-dimensional imaging of femtosecond laser-written buried structures is demonstrated using optical coherence microscopy providing lateral and depth resolution on a micron scale. This high speed technique, which requires no sample preparation, enables the visualization of volumetric structural modification created deep in transparent dielectric medium with high signal/noise contrast. Images of buried void structures with dimensions as large as 190 μm in length were obtained without shadowing effects impugning the image fidelity.

1 Introduction

Direct laser structuring of materials has been successfully employed in fields of micro-fabrication for over a decade [1–6]. Recently, the trend in laser micro-fabrication of materials has been moving from two-dimensional surface modifications towards three-dimensional volumetric structuring, responding to demands for higher-order integration [7, 8]. Femtosecond laser direct writing provides a unique means of volumetric processing with nanometer precision. Since it is based on multi-photon absorption processes [9–11], it allows the fabrication of three-dimensional structures within a transparent medium without degradation of the surface quality. Concurrent with the ability to fabricate volumetric structures in transparent media is the need for a method of high-resolution three-dimensional imaging fast enough, ultimately, to permit improvements in precision and quality of the laser machined structures in real-time. In addition, fast diagnostic feedback during the writing process will allow high-speed control of the writing parameters, enabling, for instance, consistent device fabrication across variations in material homogeneity and interfaces between materials having different processing parameters. To realize this concept, we seek a nondestructive imaging technique that possesses high optical resolution and real-time image acquisition. High resolution microscopic imaging techniques such as electron microscopy and atomic force microscopy have traditionally been used to analyze the quality of laser micro-machined surface structures [12]. However, neither of these is amenable to characterizing structures that are internally located in a transparent material. Electron microscopy is ideal for ultra-fine surface features, but often requires a multi-step sample preparation process that possibly involves vacuum encapsulation. Although simpler to use, atomic force microscopy has the same limitation and suffers from slow scanning speeds and is very sensitive to vibrations [13]. Conventional optical microscopy techniques such as confocal and fluorescence microscopy can provide three-dimensional information noninvasively. However, they are not single-step image acquisition processes allowing for real-time construction of three dimensional images and can therefore only be used for post processing evaluation. Optical coherence microscopy (OCM), a relatively new technique, has demonstrated in situ noninvasive highly-resolved three-dimensional images of biological specimens

J. Choi · J.P. Rolland · T. Anderson · M.C. Richardson (✉)
Townes Laser Institute, College of Optics and Photonics, University of Central Florida, 4000 Central Florida Blvd. Orlando, FL 32816-2700, USA
e-mail: mcr@creol.ucf.edu

K.-S. Lee · J.P. Rolland
The Institute of Optics, University of Rochester, 275 Hutchison Rd, Rochester, NY 14627, USA

J. Choi
Present address: Korea Institute of Machinery and Materials, 104 Sinseongno, Yuseong-Gu, Daejeon 305-343, Korea
e-mail: jchoi@kimm.re.kr

[14–16]. Most OCM implementations utilize femtosecond Ti:Sapphire lasers to take an advantage of their broadband spectrum. The materials of interest for 3-D laser microstructuring, such as oxide and non-oxide glasses and optical polymers, possess the same transparency window, and therefore it is possible to perform low noise measurements relying on low intrinsic extinction ratios. Optical Coherence Tomography (OCT) has previously been used to image both refractive index structures and void-like structures produced by femtosecond laser writing in glass. Minoshima et al. [17] utilized OCT for imaging the cross-section of laser-written waveguide structures produced in soda-lime glass to estimate the refractive index change of an X coupler. However, these structures were limited to within a shallow region close to the surface. Demos et al. [18] used OCT to characterize subsurface crack formation in laser induced surface defects as large as 2 mm wide generated on the surface of optical components. To our knowledge, no OCM investigations have yet been reported of deeply-buried femtosecond laser-written void structures. When these structures are used with post laser-irradiation processes such as selective etching, say for the formation of microfluidic channels, nondestructive imaging techniques such as that described here will aid the fabrication process by providing precision measurement of the structures during the writing process, enabling compensation for fabrication errors due to nonlinear optical effects such as self-focusing. Moreover, OCM imaging during the etching phase will provide high S/N imaging from the high-scattering void structures, allowing real-time moderation of the etching phase. In this paper, we describe the utilization of OCM for visualizing buried femtosecond laser-written three-dimensional voids created in fused silica with different laser irradiances. For the first time, we use this technique to visualize deeply buried laser-written void structures and make quantitative assessments of their features. The value of OCM imaging is demonstrated in measurements of the effect of self-focusing of the writing laser beam on the position of the written structure in the transparent substrate material. This allows for OCM to be used to compensate for this effect in positioning specific 3-D laser written structures at pre-determined depths to high accuracy.

2 Experiment

2.1 Formation of 3-D structures using a femtosecond laser

Microstructures consisting of void formation were produced by an ultrafast laser system coupled to a computer-controlled 3-D stage. A 1 kHz 800 nm Ti:Sapphire regenerative amplifier (Spectra Physics, Spitfire) was used to write the buried structures in fused silica. The 120 fs pulse duration was verified with a Grenouille autocorrelator (Swamp Optics, Model 8-20). The laser was integrated with a laser direct-writing system consisting of (i) a computer controlled three-dimensional writing stage (Newport, VP-25XA), (ii) a light valve comprising a half-wave plate and a cube beam polarizer to attenuate the beam power, and (iii) a microscope objective (NA = 0.15) to deliver the femtosecond beam to the sample. The focused beam size was estimated to be ~6.5 μm. Buried structures were produced in fused silica substrates mounted on the 3-D translation stage in a plane perpendicular to the beam propagation axis, the z direction in Fig. 1. The focus of the writing beam was first positioned at the surface of the substrate then moved into the substrate by moving the substrate 500 μm upward. Thus, the focused beam was placed at ~727 μm from the surface, taking into account the linear refractive index n_0 of fused silica ($n_0 = 1.453$ at 800 nm). The layer of structures generated at this location (Fig. 1) comprised an array of structures illustrated in the map shown in Fig. 2. In a preliminary step, the pulse energy and energy density to produce bulk void formation in the fused silica sample was measured to be ~4.7 μJ, corresponding to a laser fluence of 14.1 J/cm^2. With this knowledge of the energy density threshold for void formation, three-dimensional buried structures were fabricated with pulse energies varying from 1.6 to 8.3 μJ, that is from 66% below the damage threshold to 76% above it. The writing speed was kept constant at 600 μm/s so that the laser dose was governed only by laser pulse energy. In this manner, graduated changes in the material were created, either from (i) structural changes below the damage threshold, primarily a consequence of structural densification resulting from localized melting and subsequent rapid cooling, or (ii) void formation due to micro-explosion at energy densities above it [7, 19]. A series of seven 3-D box structures with sizes ranging from 10 to 100 μm wide was fabricated for

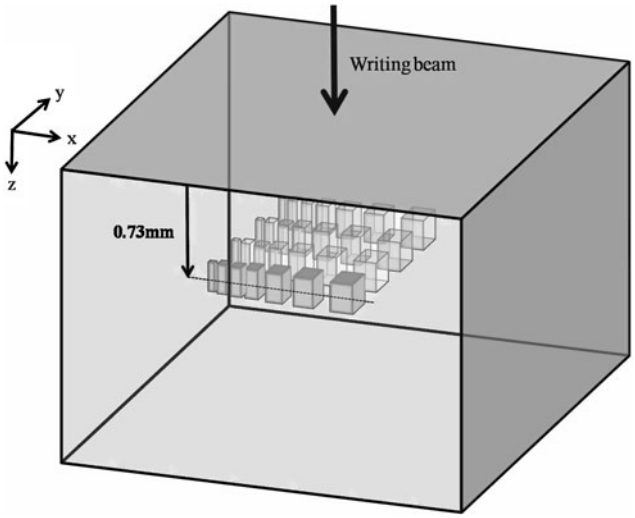

Fig. 1 3-D design of the laser direct written structures in a fused silica substrate

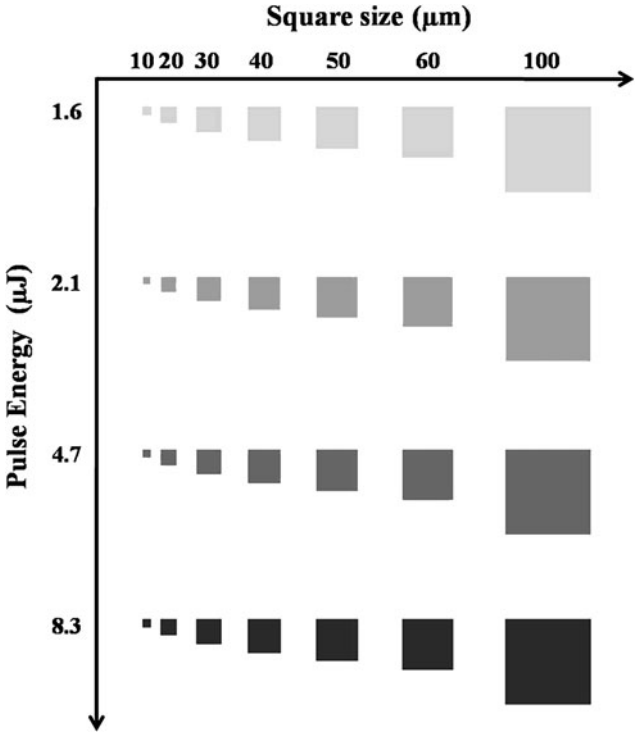

Fig. 2 Map of the written structures. The color codes in gray represent the relative strength of the laser pulse energy

each pulse energy. The squares were produced by scanning the focused laser beam perpendicular to the laser propagation direction in a raster pattern with a pitch of 2 μm (one third of the focused beam size) in the direction perpendicular to the beam propagation direction to eliminate gaps between exposed lines.

2.2 3-D image acquisition using OCM

The OCM images of the laser-written structures were obtained with a femtosecond Ti:Sapphire laser (Femtolasers Inc., Femtosource Integral OCT). Figure 3 shows the schematic of the custom built OCM system. The center wavelength and the spectral bandwidth of the source are 800 and 120 nm, respectively. The spectral bandwidth provides ∼2.5 μm axial resolution in air and ∼1.72 μm in fused silica where the axial resolution is calculated as half of the coherence length of the light source. In this imaging system, 80% of the total beam intensity from the 80:20 coupler was collimated to a 2 mm diameter beam size (full width at $1/e^2$). The collimated beam was then incident onto a 20× magnification, 0.12 NA microscope objective integrated into the sample arm of the OCM system. The light was then focused onto the sample, achieving about 4.4 μm transverse resolution with a depth of focus of approximately 35 μm in the fused silica. The remaining 20% of the beam intensity was used as a reference beam reflected by a mirror through a Fourier-domain optical delay line located in the reference

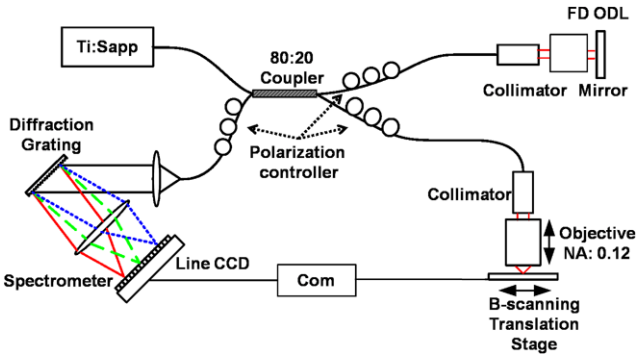

Fig. 3 Schematic diagram of the custom built OCM system

arm to control the overall dispersion in the system. The polarization was adjusted to yield maximum signal modulation contrast. A spectrometer with a 3648 CCD pixel line array (Ocean Optics Inc., HR 4000) was used as the detection system. The system sensitivity was estimated to be 97 dB. The structures in the fused silica were then examined using the custom built OCM station. The location of the focus of the probe beam was varied for different image planes in the sample to maximize lateral resolution and sensitivity throughout the imaging volume [16]. The x–y OCM images for the top view of the structures were reconstructed with a 1000×1000 μm^2 field of view, which comprised spectral datasets with 200 x–z axial image scans acquired, by slicing the three-dimensional data matrix in the x–y direction. The scanning time per line (x–z plane) was about 0.9 s/scan, and therefore the image acquisition time is primarily dependent upon the size of the structure. Since the scanning speed is faster than the writing speed for the structure, real time image acquisition is feasible. Furthermore, on-going investigations to optimize the system is greatly reducing the acquisition time, which will be the subject of a future publication. The primary intent of the present investigation is to demonstrate OCM as a diagnostic tool for deeply embedded laser written structures, and to show that online feedback during the writing process is feasible.

3 Results and discussion

One of the many advantages of OCM is the capability to portray three-dimensional images from any direction. This is of particular relevance when viewing complex microstructures deeply embedded below the surfaces of materials, where perhaps, only the top surface is polished and transparent for the processing and imaging beams, and all other surfaces are opaque. Here we demonstrate this with OCM images of the structures created in this investigation. Figure 4(a) shows the OCM reconstructed images of the side view in the x–z plane. Figures 4(b)–(d) show reconstructed images in the x–y plane observed at three different values

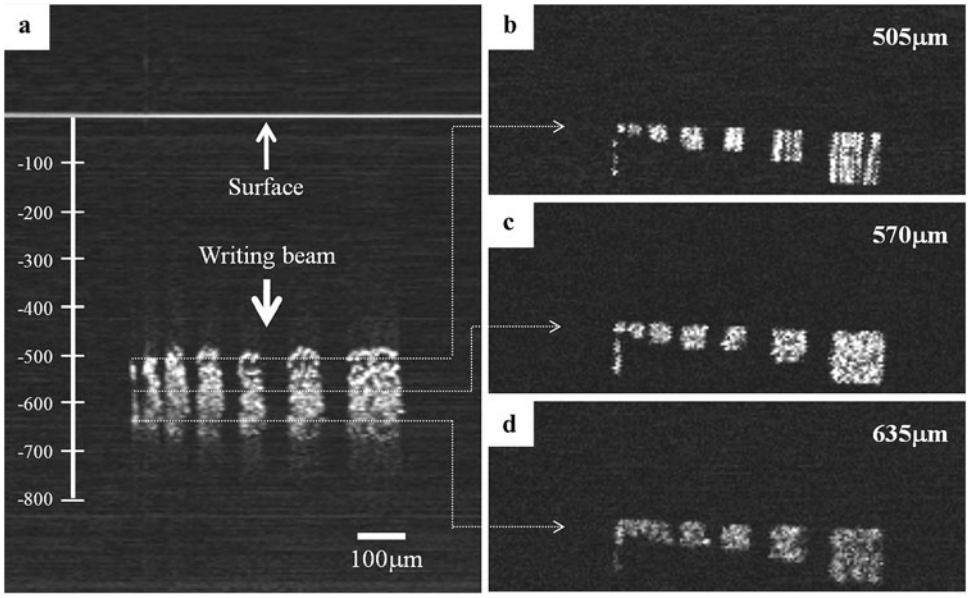

Fig. 4 **(a)–(d)** The side view of the first layer and top views acquired with OCM at 505, 570 and 635 μm from the surface

of z, (505, 570 and 635 μm, respectively), below the surface. The photo-induced void formations in the squares irradiated with 8.3 μJ are clearly visualized. It is interesting to note that although high scattering losses are expected at the top of the structure, which could cause a signal shadow that restricts acquiring an image of the entire structure, the structures are clearly visualized from top to bottom. They extend in depth along the z-axis from one end of the confocal region to the other. The OCM images provide some insight on the processes leading to void formation in the fused silica. It is observed that the center of void features is located at $z \sim 570$ μm from the surface of the sample at $z = 0$ μm, whereas the calculated focus of the structuring beam was at $z = 727$ μm. This shift in the focus of the structuring beam is a consequence of self-focusing and filamentation of the processing beam in the fused silica. The critical power for self-focusing in fused silica [10] $P_{cr} = \pi 0.61^2 \lambda^2 / 8 n_0 n_2$ is calculated to be 2.2 MW, where λ is the center wavelength of the writing laser and n_0 and n_2 are the linear and nonlinear refractive indices of fused silica, respectively ($n_2 \sim 3 \times 10^{16}$ cm^2/W) [20]. The peak power at 8.3 μJ is calculated to be ∼69.2 MW for the ∼120 fs pulse duration. Self-focusing therefore adds to geometrical focusing to reduce the position of the beam focus below the surface of the sample. To estimate the difference Δz between the focal depth without considering self-focusing and the actual focus, the self-focusing distance z_{sf} from the surface can be estimated from [10, 20]

$$z_{\mathrm{sf}} = \frac{\frac{1}{2} k w^2}{\sqrt{P/(P_{\mathrm{cr}} - 1)} + 2 z_{\mathrm{min}} / k w_0^2} \tag{1}$$

where P and P_{cr} are the peak power of the writing pulses and the critical power for self-focusing of fused silica, respectively. z_{min} is the distance from the surface to the focus of the objective lens, and w and w_0 are the beam radii at the surface and at the focused beam waist. This yields a value of $z_{sf} \sim 552$ μm and thus Δz is estimated to be ∼174 μm compared to $\Delta z \sim 157$ μm deduced from Fig. 4(a). The difference between these two values could in part be due to the dispersion of the femtosecond laser pulses in fused silica. An increase in the pulse duration to $\tau \sim 155$ fs due to the combined dispersion in the focusing lens and in the fused silica substrate would reduce the peak power to that commensurate with the change in focus position. The actual length of the void structure in the z-direction may also be affected by self-focusing. The estimated confocal length of the writing beam is ∼150 μm and with our optical parameters, the energy density would range from ∼12.5 J/cm^2 at the ends to ∼25.1 J/cm^2 in the center. However, the actual length of the cubic void, corresponding to the where the energy density is equivalent to or larger than the threshold for void formation (14.1 J/cm^2), is much longer (about ∼190 μm). This observation would also be consistent with the occurrence of self-focusing.

It is also observed that the upper and lower boundaries of the structures are not as sharp as the lateral or side boundaries. The top and bottom boundaries of the structures are at the end of the confocal region of the Rayleigh range of the writing configuration. The sample was not translated in the z-direction. The highest spatial resolution of the writing beam exists therefore at the middle of each structure. It should be noted that by imaging the side and the cross section of each structure, the amount of the structural change can easily be visualized. In the images, the density of the object is a representation of the density of the laser-induced micro-cracks resulting from voids. Figures 5(a) and 5(b) show the signal strengths of the side and

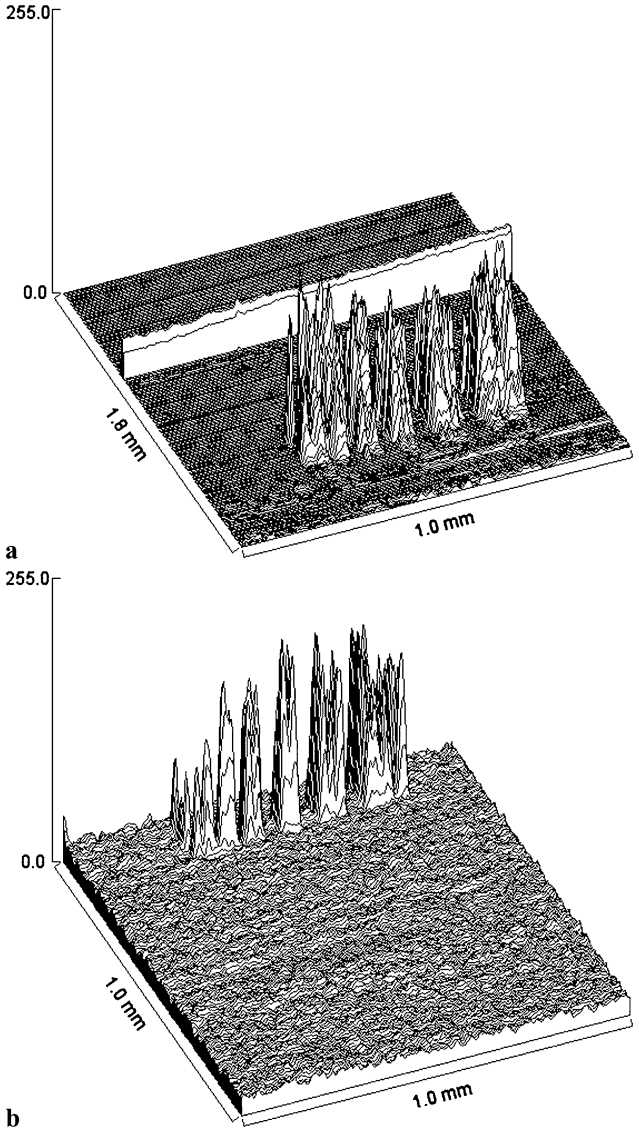

Fig. 5 Signal strength plots in gray scale of the side view **(a)** and top view **(b)** of written structures at 505 μm below the surface

top views backscattered from the laser written objects. The high signal-to-background, indicating that high-fidelity images can be retrieved by OCM, in part a consequence of the high transparency of a fused silica at 800 nm. Figure 5(a) also shows that such high signal-to-background ratio is continued throughout the modification length measuring in the z-direction, which implies that there is little or negligible shadowing effect by the scattered from the micro-cracks at the top. These findings show that OCM is a promising nondestructive method providing accurate three-dimensional information of femtosecond laser written volumetric structures with extremely low background scattering noise. Furthermore, since this technique does not require any sample preparation prior to measurement, it can be considered as a real-time diagnostic for the evaluation of the quality of laser-induced features.

4 Conclusion

We have demonstrated the use of optical coherence microscopy for nondestructive three-dimensional imaging of femtosecond laser direct written structures produced within a transparent fused silica substrate. In principal, this technique can be applied to the visualization of any structures buried deep in materials transparent to the OCM imaging wavelength. Here the three-dimensional image constructions reveal the effective volume of the buried structures produced by the femtosecond laser. The technique has revealed how self-focusing of the femtosecond laser writing beam affects the location of the void formation. With optimization of the imaging system and improvements to the image processing, this method can be implemented to control the writing parameters during the processing routine. Implementing OCM in combination with a femtosecond laser materials processing station would enable one-step micro-fabrication and nondestructive diagnosis of three-dimensional structures deeply embedded in transparent materials. This would increase the comparability of femtosecond laser micromachining techniques to photonic device fabrication.

Acknowledgements This work was supported by a contract from the National Science Foundation (ECS 0437614) and the state of Florida.

References

1. K. Venkatakrishnan, B.K.A. Ngoi, P. Stanley, L.E.N. Lim, B. Tan, N.R. Sivakumar, Appl. Phys. A **74**, 493 (2002)
2. P.P. Pronko, S.K. Dutta, J. Squier, J.V. Rudd, D. Du, G. Mourou, Opt. Commun. **114**, 106 (1995)
3. L. Shah, J. Tawney, M. Richardson, K. Richardson, Appl. Surf. Sci. **183**, 151 (2001)
4. G. Kamlage, T. Bauer, A. Ostendorf, B.N. Chichkov, Appl. Phys. A **77**, 307 (2003)
5. A. Zoubir, L. Shah, K. Richardson, M. Richardson, Appl. Phys. A **77**, 311 (2003)
6. A. Zoubir, M. Richardson, L. Canioni, A. Brocas, L. Sarger, J. Opt. Soc. Am. B **22**, 2138 (2005)
7. E.N. Glezer, E. Mazur, Appl. Phys. Lett. **71**, 882 (1997)
8. S. Juodkazis, K. Yamasaki, V. Mizeikis, S. Matsuo, H. Misawa, Appl. Phys. A **79**, 1549 (2004)
9. L.V. Keldysh, Zh. Eksp. Teor. Fiz. **47**, 1945 (1964)
10. R.W. Boyd, *Nonlinear Optics* (Academic Press, San Diego, 2008), p. 332
11. A. Zoubir, C. Rivero, R. Grodsky, K. Richardson, M. Richardson, T. Cardinal, M. Couzi, Phys. Rev. B **73**, 224117 (2006)
12. J.Y. Choi, J.G. Kim, B.S. Shin, K.H. Whang, J. Opt. Soc. Kor. **7**, 47 (2003)
13. J. Massera, J. Choi, L. Petit, M. Richardson, Y. Obeng, K. Richardson, Mater. Res. Bull. **43**, 3130 (2008)
14. J.A. Izatt, M.R. Hee, G.M. Owen, E.A. Swanson, J.G. Fujimoto, Opt. Lett. **19**, 590 (1994)
15. S. Murali, K.P. Thompson, J.P. Rolland, Opt. Lett. **34**, 145 (2009)
16. The terms OCT and OCM are often used alternately, but here we use OCM to emphasize that the structures investigated in this paper are microscopic in scale. J.P. Rolland, P. Meemon, S. Murali, K.P. Thompson, K.S. Lee, Opt. Express **18**, 3632 (2010)

17. K. Minoshima, A.M. Kowalevicz, I. Hartl, E.P. Ippen, J.G. Fujimoto, Opt. Lett. **26**, 1516 (2001)
18. S.G. Demos, M. Staggs, K. Minoshima, J. Fujimoto, Opt. Express **10**, 1444 (2002)
19. K. Miura, J. Qiu, H. Inouye, T. Mitsuyu, K. Hirao, Appl. Phys. Lett. **71**, 3329 (1997)
20. A. Saliminia, N.T. Nguyen, S.L. Chin, R. Vallée, Opt. Commun. **241**, 529 (2004)